Hindawi
Geofluids
Volume 2022, Article ID 2206989, 6 pages
https://doi.org/10.1155/2022/2206989

Research Article

Determination of the Fractal Dimension of CO_2 Adsorption Isotherms on Shale Samples

Hongyan Qi, Zhenlin Wang, Jianglong Yu, Peirong Yu, and Guoqing Zheng

Petro China Xinjiang Oilfield Company, Karamay 834000, China

Correspondence should be addressed to Zhenlin Wang; wzhenl@petrochina.com.cn

Received 19 January 2022; Accepted 31 January 2022; Published 22 February 2022

Academic Editor: Kouqi Liu

The fractal theory has been widely applied to the analysis of gas adsorption isotherms, which are used for the pore structure characterization in unconventional reservoirs. Fractal dimension is a key parameter that can indicate the complexity of the pore structures. So far, most fractal models for gas adsorption are for N_2 adsorption, while fractal models for CO_2 adsorption are rarely reported. In this paper, we built a fractal model for CO_2 adsorption by combining a thermodynamic model and the Dubinin–Astakhov model. We then applied the new model to three CO_2 adsorption isotherms measured on shale samples. The results show that the fractal dimension from the new model lies between 2 and 3, which agrees with the fractal geometry. The new model presented in this paper can be used for the CO_2 adsorption analysis, which allows characterizing micropore structures in shales.

1. Introduction

Knowing the pore structures of shale rocks is an essential part for the reservoir characterization which could assist in understanding the original oil/gas in place and the flow characteristics of the shale rocks [1–3]. The gas adsorption method is now a standard method for pore strcuture correction. The gas adsorption method involves bringing the gas/vapor into contact with the solid surface [4–6]. For shale rocks, N_2 and CO_2 are the two gases that are typically used for gas adsorption. N_2 adsorption (at 77 k) can be used to derive the specific surface area (using the Brunauer, Emmett, and Teller equation) and pore size distribution (using the Barrett–Joyner–Halenda model or density functional theory) [7, 8]. N_2 adsorption can mainly get the meso-macropore information (pore size >2 nm) and cannot provide the micropore information. Under low temperature, the N_2 molecule is kinetically restricted from accessing the micropores [9]. In order to overcome the limitations of N_2 adsorption, CO_2 adsorption is commonly performed. The critical dimensions of the CO_2 molecule and the N_2 molecule are very similar (0.28 nm for CO_2 and 0.30 nm for N_2), but the higher working temperature for CO_2 adsorption (273 k for CO_2 adsorption) helps the CO_2 molecule to enter into the micropores [9]. CO_2 adsorption (273 k) is usually complemented by the N_2 adsorption (77 K) to get a wider pore size information in shale reservoir characterization.

The pore structure of shale samples is very complicated, which has been shown by many researchers using the scanning electron microscope [10–15]. In order to understand the complexity of the pore structures, the fractal theory can be applied. Avnir et al. [16] found that at the molecular level, the surface of most materials has a fractal behavior with fractal dimension varying from 2 to 3, where 2 means a perfectly smooth surface and 3 denotes significantly rough and a disordered surface. Several fractal models have been developed for N_2 adsorption, such as the Frenkel–Halsey–Hill (FHH) theory [17] or the thermodynamic model by Neimark [18]. These models for N_2 adsorption are mainly focused on the meso-macro pore (>2 μm) capillary condensation by using Kelvin's equation. However, Kelvin's equation is not valid for the pores with sizes smaller than 7.5 nm [19], which indicates that these current fractal models cannot be used for CO_2 adsorption. Most researchers only analyzed the fractal dimension from the N_2 adsorption, even when they performed both N_2 adsorption and CO_2 adsorption experiments [3, 20, 21]. To the best of the authors' knowledge, the fractal model for the CO_2 adsorption in shale

studies has not been yet reported. In this paper, we present a fractal model for CO_2 adsorption built by combining the thermodynamic model and the Dubinin–Astakhov analysis model.

2. Model Description

From the thermodynamic viewpoint, the differential of the interface area ds can be calculated from the balance between the work of forming the interface and the work from the adsorption of CO_2 [18]:

$$\sigma \mathrm{d}s = \Delta\mu \mathrm{d}N, \tag{1}$$

where σ is the surface tension, μ is the differential chemical potential of CO_2, and N is the adsorption amount of CO_2.

For CO_2, the differential chemical potential under pressure p can be calculated using the following equation [22, 23]:

$$\Delta\mu = RT \ln \frac{p}{p_0}, \tag{2}$$

where R is the universal gas constant, 8.314 $\mathrm{Jmol^{-1}K^{-1}}$; T is the temperature, 273 K; p is the working pressure; and p_0 is the CO_2 saturation pressure under 273 K.

By combing equations (1) and (2), we can obtain the following equation:

$$S = \frac{1}{\sigma} \int_{N_{p/p_0}}^{N_{\max}} RT \ln \frac{p}{p_0} \mathrm{d}N, \tag{3}$$

where $N_{\max}$ is the maximum cumulative adsorption quantity and $N_{(p/p0)}$ is the cumulative adsorption quantity under the relative pressure ($p/p0$).

The correlation of the area for a fractal surface and the volume circumscribed by the surface obeys the following equation [24]:

$$S^{1/D} \sim V^{1/3}, \tag{4}$$

where D is the fractal dimension.

If the fractal surface is measured on a Euclidean area, equation (4) can be changed to the following equation by the dimensional analysis [25]:

$$S = k^D r^{2-D} V^{D/3}, \tag{5}$$

where k is a correlation factor between the surface and the volume, r is the radius, and V is the volume.

Assuming that the gas molecules cannot be compressed, the volume can be calculated using the following equation:

$$V = \left(N_{\max} - N_{N_{p/p_0}}\right) V_L, \tag{6}$$

where V_L is the molecular volume of CO_2.

By combining equations (3) and (6), we obtain the following expression:

$$\frac{1}{\sigma} \int_{N_{p/p_0}}^{N_{\max}} RT \ln \frac{p}{p_0} \mathrm{d}N = k^D r_{p/p_0}^{2-D} \left(N_{\max} - N_{p/p_0}\right)^{D/3} V_L^{D/3}, \tag{7}$$

which can be further rewritten as

$$\frac{\int_{N_{p/p_0}}^{N_{\max}} \ln\ (p/p_0)\mathrm{d}N}{r_{p/p_0}^2} = \frac{\sigma}{RT} k^D V_L^{D/3} \left[\frac{N_{\max} - N(p/p_0)}{r_{p/p_0}}\right]^D, \tag{8}$$

where $r_{p/p0}$ is the pore radius under the relative pressure $p/p0$.

The form of equation (8) is similar to the equation which was provided by Wang and Li [25] for the N_2 adsorption analysis. However, in their model, they applied the Kelvin equation to obtain the pore radius for the mesopore capillary condensation stage, which is not suitable for the micropores. For the micropores, $r_{p/p0}$ can be derived from the Dubinin–Astakhov model [26]:

$$\frac{W}{W_0} = \exp\left[-\left(\frac{-RT \ln(p/p_0)}{E}\right)^n\right], \tag{9}$$

where w_0 is the limiting adsorption volume, w is the occupied adsorption volume, E is the characteristic energy of the system, and n is an empirical constant.

Then, the pore size of the sample can be calculated using the following equation:

$$\frac{\mathrm{d}(W/W_0)}{\mathrm{d}r_{p/p_0}} = 3n\left(\frac{D_0}{E}\right)^n r_{p/p_0}^{-(3n+1)} \exp\left[-\left(\frac{D_0}{E}\right)^n r_{p/p_0}^{-3n}\right], \tag{10}$$

where D_0 is the dispersion interaction energy.

If we combine equations (9) and (10), we can express the radius:

$$r_{p/p_0} = \left(\frac{-RT \ln(p/p_0)}{D_0}\right)^{-1/3}. \tag{11}$$

For equation (8), let $A_{p/p_0} = \ln(\int_{N_{p/p_0}}^{N_{\max}} \ln\ (p/p_0)\mathrm{d}N/r_{p/p_0}^2)$ and $B_{p/p_0} = \ln((N_{\max} - N(p/p_0))/r_{p/p_0})$; then, equation (8) can be written in the following form:

$$A_{p/p_0} = C + DB_{p/p_0}. \tag{12}$$

Thus, if A and B values are calculated under different relative pressure for a CO_2 adsorption isotherm, then the fractal dimension D can be easily determined from the slope of the function in equation (12). C is a constant which can be derived from curve fitting.

3. Results and Discussion

3.1. Model Verification. In order to verify this model, we performed the CO_2 adsorption experiment on three shale samples and calculated their fractal dimension using equation (12). Figure 1 shows the adsorption isotherms of the three samples (the relative pressure is from 0.001 to 0.03).

3.2. Impact of D_0 on the Results. We applied the new model to calculate the A and B values of each sample under different relative pressure values and then plot A as a function of B (Figure 2) (here, we assume that D_0 is 1500 $\mathrm{Jnm^3mol^{-1}}$, from Hiden Isochema). Very strong linear relations exist between A and B for all three samples, indicating that the CO_2 adsorption isotherm shows the fractal behavior. The fractal

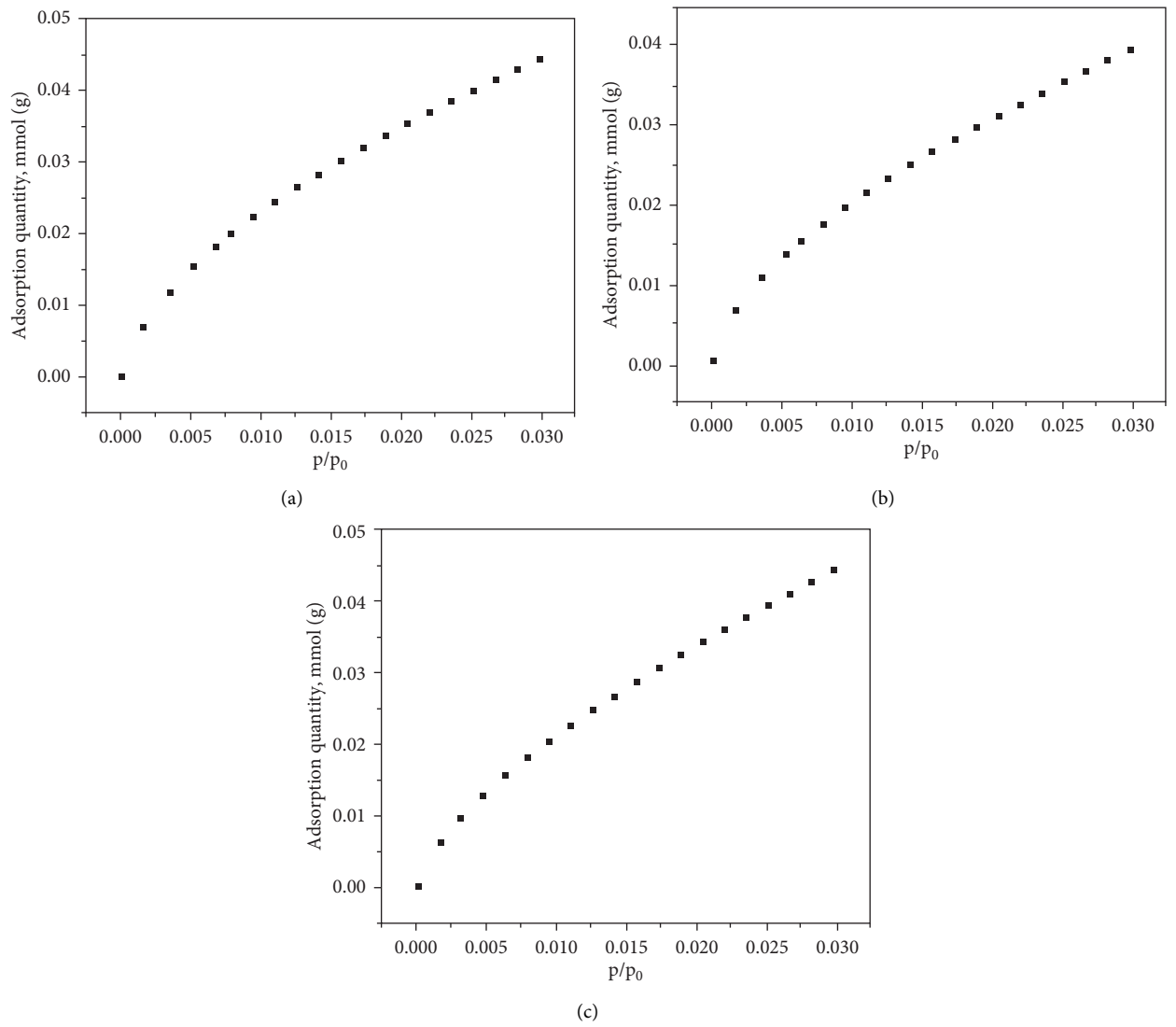

Figure 1: Measured CO_2 adsorption isotherms of three shale samples. (a) Sample 1. (b) Sample 2. (c) Sample 3.

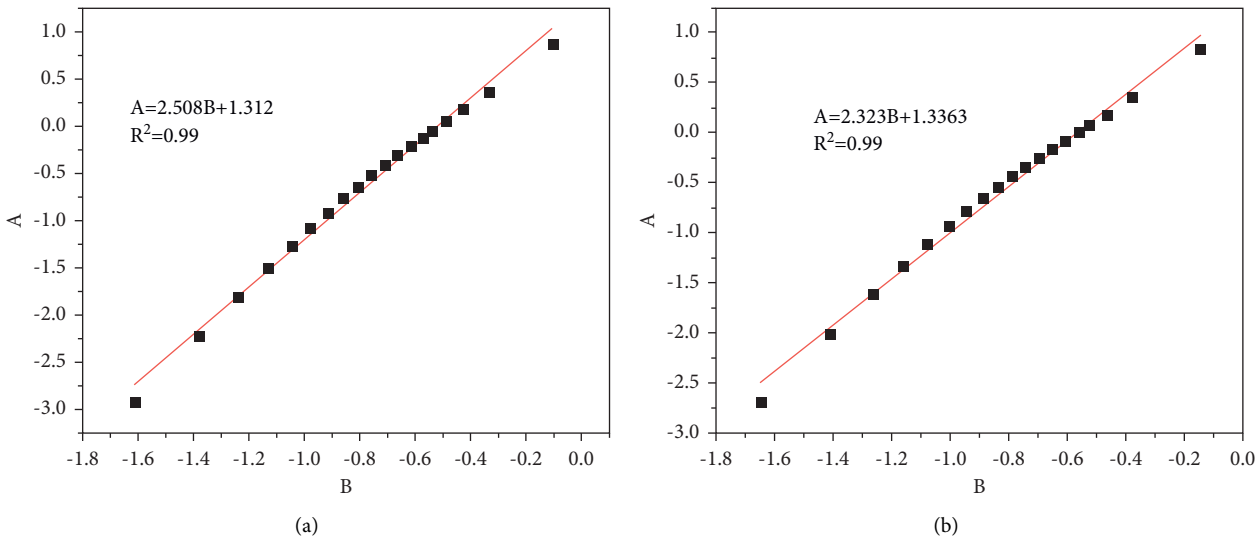

Figure 2: Continued.

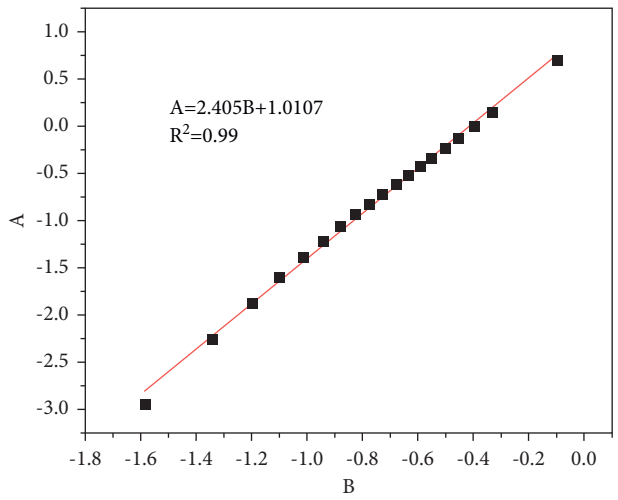

(c)

Figure 2: Fractal analysis of the CO_2 adsorption isotherms of the three shale samples. (a) Sample 1. (b) Sample 2. (c) Sample 3.

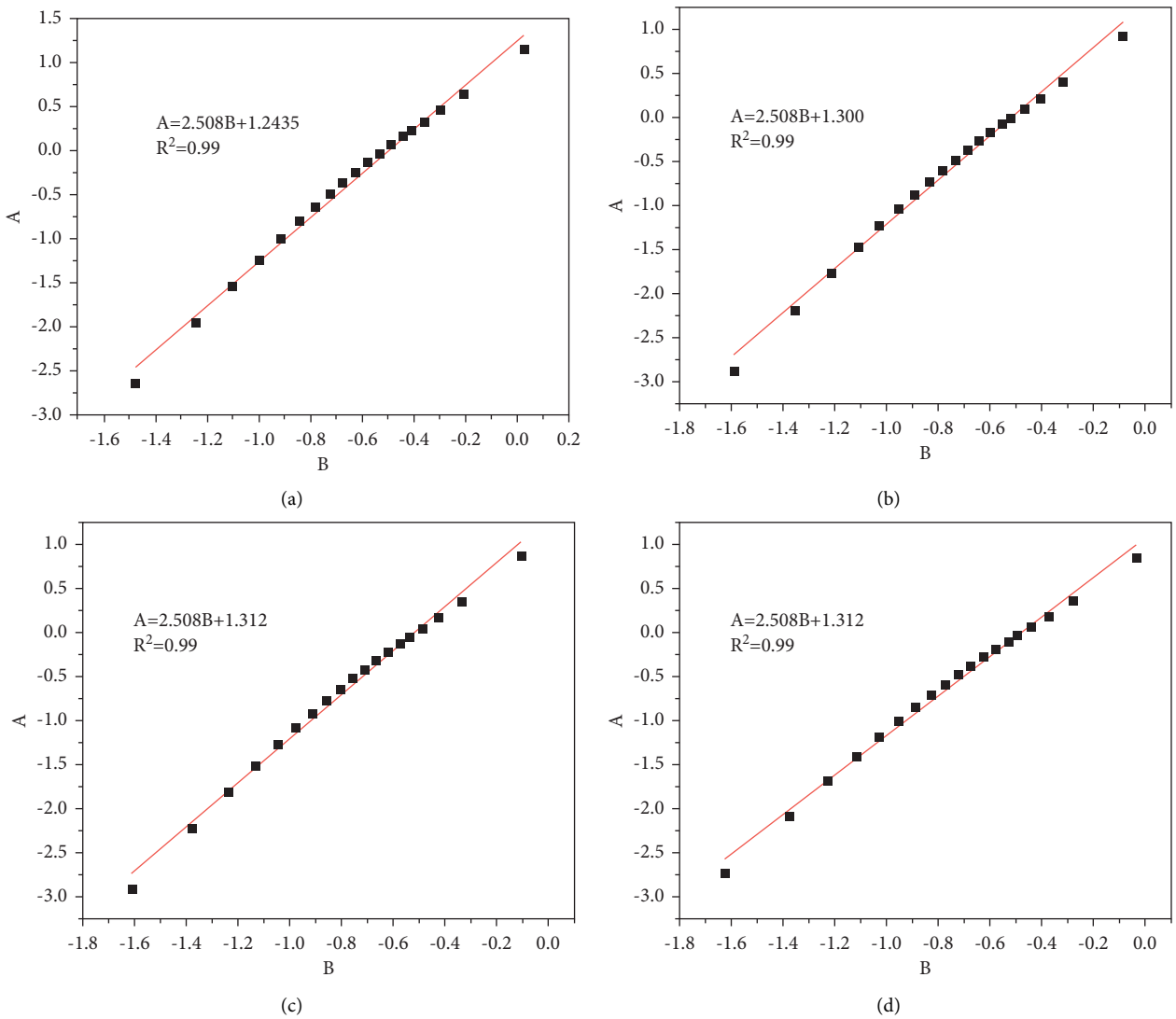

(a)

(b)

(c)

(d)

Figure 3: Continued.

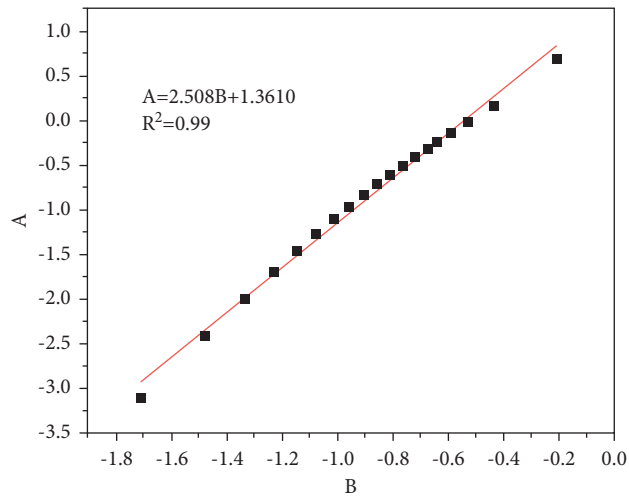

(e)

FIGURE 3: The impact of D_0 on the fractal dimension (sample 1). (a) $D_0 = 1000\ \text{Jnm}^3\text{mol}^{-1}$. (b) $D_0 = 1400\ \text{Jnm}^3\text{mol}^{-1}$. (c) $D_0 = 1500\ \text{Jnm}^3\text{mol}^{-1}$. (d) $D_0 = 1600\ \text{Jnm}^3\text{mol}^{-1}$. (e) $D_0 = 2000\ \text{Jnm}^3\text{mol}^{-1}$.

dimensions of these three samples are 2.508, 2.323, and 2.405, respectively. The fractal dimension falls within the expected range of $2 < D < 3$, predicted by the fractal geometry [25, 27]. Thus, the model yields robust results and can be used to calculate the fractal dimension of CO_2 adsorption on shale samples.

In the previous examples, we had to assume a value for D_0 in order to calculate $r_{p/p0}$. D_0 is the dispersion interaction energy of CO_2, which is not well constrained but is usually set to around $1500\ \text{Jnm}^3\text{mol}^{-1}$ [28]. In this part, we further studied the effect of D_0 value on the fractal dimension. We set three D_0 values (1000, 1400, 1500, 1600, and $2000\ \text{Jnm}^3\text{mol}^{-1}$) and then calculated the fractal dimension of sample 1 for all three cases. Figure 3 shows that the absolute values of the A and B values do vary for different D_0, but the slope of the linear regression of A to B remains the same. Therefore, the choice of D_0 value does not affect the fractal dimension calculation. The fractal dimension value of the CO_2 adsorption isotherm from shale samples can be derived even when the exact D_0 value is not well constrained.

3.3. Future Research. Clay bound water is an important factor that could affect the fractal dimensions of the gas adsorption which has been studied by many researchers [29–31]. Under different moisture content, the fractal dimension changes. However, in this study, we preheated the samples under 105°C for over 12 hours and we believe that the effect of the clay bound water effect can be neglected. In this study, our focus is to derive a model to describe the fractal model for the analyzing the fractal dimensions of the CO_2 gas adsorption. Thus, the samples we choose are from a single basin and very simple. More samples from the different shale basins will be collected and analyzed to verify the applicability of this model. In addition, based on the studies by other researchers, the fractal dimension from N_2 gas adsorption could be correlated with the pore structures [32]. Whether the fractal dimension from CO_2 gas adsorption is correlated with the microstructures of the samples and how the microstructures affect the fractal dimension will be the target for the next step research.

4. Conclusions

(1) Based on the Dubinin–Astakhov analysis model and the thermodynamic model, we built the fractal analysis model for CO_2 adsorption on shale samples.

(2) We applied the new model to calculate the fractal dimensions of the CO_2 adsorption isotherms for three shale samples. We found that the CO_2 adsorption isotherms had the fractal behavior, and the fractal dimension value was between 2 and 3. This agrees with the fractal geometry and indicates the robust performance of the new model.

(3) We conducted a sensitivity analysis to investigate the effect of the dispersion interaction energy D_0 on the fractal dimension calculation and demonstrated that the choice of the D_0 value does not affect the model outcomes.

Data Availability

The data used to support the findings of this study are available from the corresponding author upon request.

Conflicts of Interest

The authors declare that they have no conflicts of interest.

Acknowledgments

The authors appreciate PetroChina Xinjiang Oilfield Company and shale oil research team. This study was supported by the Forward-Looking Basic Projects of CNPC (grant no. 2021DJ1803).

References

[1] R. M. Bustin, A. M. Bustin, A. Cui, D. Ross, and V. M. Pathi, "Impact of shale properties on pore structure and storage characteristics," in *Proceedings of the SPE Shale Gas Production Conference*, November 2008.

[2] C. R. Clarkson, N. Solano, R. M. Bustin, A. M. M. Bustin, and G. R. L. Chalmers, "Pore structure characterization of North American shale gas reservoirs using USANS/SANS, gas adsorption, and mercury intrusion," *Fuel*, vol. 103, pp. 606–616, 2013.

[3] K. Liu, M. Ostadhassan, J. Zhou, T. Gentzis, and R. Rezaee, "Nanoscale pore structure characterization of the bakken shale in the USA," *Fuel*, vol. 209, pp. 567–578, 2017.

[4] L. M. Anovitz and D. R. Cole, "Characterization and analysis of porosity and pore structures," *Reviews in Mineralogy and Geochemistry*, vol. 80, no. 1, pp. 61–164, 2015.

[5] S. Scaife, P. Kluson, and N. Quirke, "Characterization of porous materials by gas adsorption: do different molecular probes give different pore structures?" *The Journal of Physical Chemistry B*, vol. 104, no. 2, pp. 313–318, 2000.

[6] K. S. Sing, "Adsorption methods for the characterization of porous materials," *Advances in Colloid and Interface Science*, vol. 76, pp. 3–11, 1998.

[7] M. Jaroniec, M. Kruk, and J. Choma, "The 50th anniversary of the barrett-joyner-halenda method for mesopore size analysis: critical appraisal and future perspectives," *Fundamentals of Adsorption*, vol. 7, pp. 570–577, 2001.

[8] P. I. Ravikovitch, A. Vishnyakov, and A. V. Neimark, "Density functional theories and molecular simulations of adsorption and phase transitions in nanopores," *Physical Review E*, vol. 64, no. 1, Article ID 011602, 2001.

[9] J. Garrido, A. Linares-Solano, J. M. Martin-Martinez, M. Molina-Sabio, F. Rodriguez-Reinoso, and R. Torregrosa, "Use of nitrogen vs. carbon dioxide in the characterization of activated carbons," *Langmuir*, vol. 3, no. 1, pp. 76–81, 1987.

[10] R. G. Loucks, R. M. Reed, S. C. Ruppel, and D. M. Jarvie, "Morphology, genesis, and distribution of nanometer-scale pores in siliceous mudstones of the Mississippian Barnett Shale," *Journal of Sedimentary Research*, vol. 79, no. 12, pp. 848–861, 2009.

[11] R. G. Loucks, R. M. Reed, S. C. Ruppel, and U. Hammes, "Spectrum of pore types and networks in mudrocks and a descriptive classification for matrix-related mudrock pores," *AAPG Bulletin*, vol. 96, no. 6, pp. 1071–1098, 2012.

[12] M. E. Curtis, R. J. Ambrose, and C. H. Sondergeld, "Structural characterization of gas shales on the micro-and nano-scales," in *Proceedings of the Canadian unconventional resources and international petroleum conference*, Society of Petroleum Engineers, Calgary, Canada, October 2010.

[13] S. Kelly, H. El-Sobky, C. Torres-Verdin, and M. T. Balhoff, "Assessing the utility of FIB-SEM images for shale digital rock physics," *Advances in Water Resources*, vol. 95, pp. 302–316, 2016.

[14] A. Golparvar, Y. Zhou, K. Wu, J. Ma, and Z. Yu, "A comprehensive review of pore scale modeling methodologies for multiphase flow in porous media," *Advances in Geo-Energy Research*, vol. 2, no. 4, pp. 418–440, 2018.

[15] Y. Yang, J. Liu, J. Yao, J. Kou, Z. Li, and T. Wu, "Adsorption behaviors of shale oil in kerogen slit by molecular simulation," *Chemical Engineering Journal*, vol. 387, Article ID 124054, 2020.

[16] D. Avnir, D. Farin, and P. Pfeifer, "Molecular fractal surfaces," *Nature*, vol. 308, no. 5956, p. 261, 1984.

[17] P. Pfeifer, "Fractal dimension as working tool for surface-roughness problems," *Applications of Surface Science*, vol. 18, no. 1-2, pp. 146–164, 1984.

[18] A. Neimark, "A new approach to the determination of the surface fractal dimension of porous solids," *Physica A: Statistical Mechanics and its Applications*, vol. 191, no. 1-4, pp. 258–262, 1992.

[19] R. T. Yang, *Adsorbents: Fundamentals and Applications*, John Wiley & Sons, Hoboken, NJ, USA, 2003.

[20] R. Yang, S. He, J. Yi, and Q. Hu, "Nano-scale pore structure and fractal dimension of organic-rich Wufeng-Longmaxi shale from Jiaoshiba area, sichuan basin: investigations using FE-SEM, gas adsorption and helium pycnometry," *Marine and Petroleum Geology*, vol. 70, pp. 27–45, 2016.

[21] X. Wang, Z. Jiang, S. Jiang et al., "Full-scale pore structure and fractal dimension of the Longmaxi shale from the Southern Sichuan Basin: investigations using FE-SEM, gas adsorption and mercury intrusion porosimetry," *Minerals*, vol. 9, no. 9, p. 543, 2019.

[22] V. K. Dobruskin, "Micropore volume filling. A condensation approximation approach as a foundation to the Dubinin–Astakhov equation," *Langmuir*, vol. 14, no. 14, pp. 3840–3846, 1998.

[23] T. T. Trinh, D. Bedeaux, J. M. Simon, and S. Kjelstrup, "Calculation of the chemical potential and the activity coefficient of two layers of CO 2 adsorbed on a graphite surface," *Physical Chemistry Chemical Physics*, vol. 17, no. 2, pp. 1226–1233, 2015.

[24] B. B. Mandelbrot, *The Fractal Geometry of Nature*, p. 109, Freeman, Dallas, TX, USA, 1982.

[25] F. Wang and S. Li, "Determination of the surface fractal dimension for porous media by capillary condensation," *Industrial & Engineering Chemistry Research*, vol. 36, no. 5, pp. 1598–1602, 1997.

[26] M. M. Dubinin and V. A. Astakhov, "Molecular sieve. Zeolites II," *Journal of the American Chemical Society*, vol. 102, p. 69, 1971.

[27] J. Lai, G. Wang, Z. Fan, Z. Zhou, J. Chen, and S. Wang, "Fractal analysis of tight shaly sandstones using nuclear magnetic resonance measurements," *AAPG Bulletin*, vol. 102, no. 2, pp. 175–193, 2018.

[28] Hiden Isochema Laboratory, "The determination of the pore size distribution of an activated carbon using Dubinin-Astakhov analysis of CO2 adsorption at 273 K," 2016, https://hidenisochema.com/content/uploads/2016/04/Hiden-Isochema-Application-Note-126.pdf.

[29] Y. Yuan, R. Rezaee, M. Verrall, S. Y. Hu, J. Zou, and N. Testmanti, "Pore characterization and clay bound water assessment in shale with a combination of NMR and low-pressure nitrogen gas adsorption," *International Journal of Coal Geology*, vol. 194, pp. 11–21, 2018.

[30] Y. Yuan and R. Rezaee, "Fractal analysis of the pore structure for clay bound water and potential gas storage in shales based on NMR and N_2 gas adsorption," *Journal of Petroleum Science and Engineering*, vol. 177, pp. 756–765, 2019.

[31] K. Liu, Z. Jin, L. Zeng, Y. Yuan, and M. Ostadhassan, "Determination of clay bound water in shales from NMR signals: the fractal theory," *Energy & Fuels*, vol. 35, no. 22, pp. 18406–18413, 2021.

[32] K. Liu, N. Zakharova, T. Gentzis, A. Adeyilola, H. Carvajal-Ortiz, and H. Fowler, "Microstructure characterization of a biogenic shale gas formation—insights from the antrim shale, Michigan basin," *Journal of Earth Science*, vol. 31, no. 6, pp. 1229–1240, 2020.